Density-functional theory for fluid-solid and solid-solid phase transitions

Atul S. Bharadwaj and Yashwant Singh
Department of Physics, Banaras Hindu University, Varanasi 221 005, India
(Received 24 December 2016; published 9 March 2017)

We develop a theory to describe solid-solid phase transitions. The density functional formalism of classical statistical mechanics is used to find an exact expression for the difference in the grand thermodynamic potentials of the two coexisting phases. The expression involves both the symmetry conserving and the symmetry broken parts of the direct pair correlation function. The theory is used to calculate phase diagram of systems of soft spheres interacting via inverse power potentials $u(r) = \epsilon(\sigma/r)^n$, where parameter n measures softness of the potential. We find that for $1/n < 0.154$ systems freeze into the face centered cubic (fcc) structure while for $1/n \geqslant 0.154$ the body-centred-cubic (bcc) structure is preferred. The bcc structure transforms into the fcc structure upon increasing the density. The calculated phase diagram is in good agreement with the one found from molecular simulations.

DOI: 10.1103/PhysRevE.95.032120

I. INTRODUCTION

Considerable efforts have been made over several decades to develop a first-principles theory that can predict the phase diagram of a system interacting via known interparticle interactions [1]. Most of these efforts have, however, been limited to finding the fluid-solid phase boundary [2–4]. Many real as well as model systems are known to have more than one crystalline solid phase. The phase diagrams of such systems have therefore one or more solid-solid phase boundaries in addition to the fluid-solid boundary. The well known example is of water, whose pressure-temperature (P-T) phase diagram has several solid-solid phase boundaries and triple points [5]. Most metallic elements on the left-hand side of the periodic group together with all the lanthanides and actinides are found to freeze at low pressures into a body-centred-cubic (bcc) structure and transform to other structures at higher pressures [6]. Model systems with sufficiently soft repulsive interactions also show similar behavior [7].

The computational study of a variety of model systems [7–10] has led researchers to derive a fundamental link between the macroscopic phase behavior and the interparticle interactions. In the case of particles interacting via spherically symmetric potentials it is found that the crystalline structure that emerges at the freezing point is predominantly controlled by the nature of the repulsive component of the interparticle potential. Harsh repulsion favors a compact structure such as the face-centred-cubic (fcc) or the hexagonal-closed-packed (hcp) structures whereas soft repulsion favors a relatively open structure such as bcc. The open structure transforms into one of the compact structures at higher pressure.

While fluid is isotropic and homogeneous, a crystalline solid is highly inhomogeneous system with sharp peaks in the one-particle density distribution $\rho(\vec{r})$ at the lattice sites, and values falling to essentially zero in the interstitial region. The thermodynamic potentials and correlation functions of a crystal are functionals of $\rho(\vec{r})$ whereas those of the fluid are simply a function of fluid density ρ_f ($=\frac{N_f}{V}$, N_f being the number of particles in volume V). The density functional formalism of classical statistical mechanics can be used to write expressions for the thermodynamic potentials of an inhomogeneous system in terms of correlation functions. The functional derivatives of the reduced Helmholtz free energy $A[\rho]$ with respect to $\rho(\vec{r})$ are related to the direct correlation functions of the system [4,11].

An exact expression for $A[\rho]$ can be found by double functional integrations in the density space of a relation that connects the second functional derivative of $A[\rho]$ with respect to $\rho(\vec{r})$ to the direct pair correlation function (DPCF) [see Eq. (2.3)]. The resulting expression involves both the symmetry conserving and the symmetry broken parts of the DPCF [12,13]. The symmetry broken part takes care of the specificity of the inhomogeneity of the crystalline structure [13]. This free energy functional has been used to study the fluid-solid transition in several model systems in two and three dimensions [13–17]. Results found for freezing parameters and the crystalline structures that emerge at the fluid-solid transition point are in very good agreement with simulation results in all cases.

In this paper we extend the theory to describe solid-solid transitions. This enables us to calculate full phase diagrams showing regions of fluid and crystalline phases. The paper is organized as follows: In Sec. II we describe a theory that uses a density functional formalism to write the exact expression for the difference in the grand thermodynamic potentials of the two coexisting phases. In Sec. III we calculate and report results for the fluid-solid and the solid-solid transitions in systems interacting via inverse power potentials. The calculated phase diagram is compared with results found from computer simulations. The paper ends with a brief summary and conclusion given in Sec. IV.

II. THEORY

In a symmetry broken phase such as a crystal, the correlation functions are the sum of two qualitatively different contributions: one that preserves the continuous symmetry of the fluid and one that breaks it and vanishes in the fluid [12,13]. Thus, for the DPCF in a crystal, we write

$$c(\vec{r}_1,\vec{r}_2) = c^{(0)}(|\vec{r}_2 - \vec{r}_1|;\rho) + c^{(b)}(\vec{r}_1,\vec{r}_2;[\rho]), \qquad (2.1)$$

where $c^{(0)}$ and $c^{(b)}$ represent, respectively, the symmetry conserving and the symmetry broken contributions. While $c^{(0)}$ depends on the magnitude of interparticle separation

$r = |\vec{r}_2 - \vec{r}_1|$ and is function of average density ρ, $c^{(b)}$ depends on both position vectors, $\vec{r}_1$ and $\vec{r}_2$, and is a functional of $\rho(\vec{r})$ (indicated by square brackets). Because of crystal symmetry, $c^{(b)}$ is invariant only under a discrete set of translations corresponding to lattice vectors $\vec{R}_i$, and can be expressed as

$$c^{(b)}(\vec{r}_1,\vec{r}_2;[\rho]) = \sum_K e^{i\vec{K}\cdot\vec{r}_c} c^{(K)}(\vec{r}), \tag{2.2}$$

where $\vec{r}_c = \frac{1}{2}(\vec{r}_1 + \vec{r}_2)$ is a center-of-mass variable, $\vec{r} = \vec{r}_2 - \vec{r}_1$ a difference variable, and $\vec{K}$ reciprocal lattice vectors (RLVs) of the crystal. Since $c^{(K)}(\vec{r})$ is real and symmetric with respect to interchange of $\vec{r}_1$ and $\vec{r}_2$,

$$c^{(-K)}(\vec{r}) = c^{(K)}(\vec{r}) \quad \text{and} \quad c^{(K)}(-\vec{r}) = c^{(K)}(\vec{r}).$$

An exact expression for the reduced free energy $A[\rho]$ is found by double functional integrations in density space of the relation [13]

$$\frac{\delta^2 A[\rho]}{\delta\rho(\vec{r}_1)\delta\rho(\vec{r}_2)} = \frac{\delta(\vec{r}_1 - \vec{r}_2)}{\rho(\vec{r}_1)} - c^{(0)}(|\vec{r}_2 - \vec{r}_1|;\rho) - c^{(b)}(\vec{r}_1,\vec{r}_2;[\rho]), \tag{2.3}$$

where δ is the Dirac delta function. The first term on the right-hand side of (2.3) corresponds to the ideal gas and is integrated analytically. The second term, which corresponds to the symmetry conserving contribution is integrated using a homogeneous system as a reference system. The third term which corresponds to the symmetry broken contribution is integrated in density space along a path defined by parameters which raise the number density and the order parameters [see Eq. (2.6)] from zero to their final values.

To locate the transition one uses the grand thermodynamic potential defined as

$$-W = A[\rho] - \beta\mu \int d\vec{r}\, \rho(\vec{r}), \tag{2.4}$$

where μ is the chemical potential and β the inverse temperature in units of the Boltzmann constant k_B. At the transition point $\mu_1 = \mu_2$ and $\Delta W = W_1 - W_2 = 0$, where subscripts 1 and 2 refer to two coexisting phases.

A. Fluid-solid transition

For the fluid-solid transition the symmetry conserving contribution is found by using the coexisting fluid which has same value of chemical potential as the solid, as the reference system. The functional integration of (2.3) leads to following expression for $\Delta W_{fc} = W_f - W_c$, where subscripts f and c refer, respectively, to the fluid and the crystal [13–17]:

$$\Delta W_{fc} = \int d\vec{r}\left[\rho_c(\vec{r})\ln\frac{\rho_c(\vec{r})}{\rho_f} - [\rho_c(\vec{r}) - \rho_f]\right] - \frac{1}{2}\int d\vec{r}_1 \int d\vec{r}_2 [\rho_c(\vec{r}_1) - \rho_f][\rho_c(\vec{r}_2) - \rho_f]c^{(0)}(r,\rho_f) - \int d\vec{r}_1 \int d\vec{r}_2 [\rho_c(\vec{r}_1) - \rho_c][\rho_c(\vec{r}_2) - \rho_c]\bar{c}_c^{(b)}(\vec{r}_1,\vec{r}_2), \tag{2.5}$$

where

$$\bar{c}_c^{(b)}(\vec{r}_1,\vec{r}_2) = 2\int_0^1 d\lambda(1-\lambda)\int_0^1 d\xi(1-\xi)c_c^{(b)} \times (\vec{r}_1,\vec{r}_2;\lambda\rho_c,\xi\rho_K). \tag{2.6}$$

Here ρ_f is density of the coexisting fluid and $\rho_c(\vec{r})$ is the single-particle density distribution of the crystal formed at the freezing point. The function $\rho_c(\vec{r})$ can be expanded in Fourier series as

$$\rho_c(\vec{r}) = \rho_c + \sum_K \rho_K e^{i\vec{K}\cdot\vec{r}}, \tag{2.7}$$

where $\rho_c = \rho_f(1 + \Delta\rho^*)$ is the average density of the crystal, $\Delta\rho^*$ is the relative change in density upon freezing, ρ_K are the order parameters, and $\vec{K}$ are the RLVs of the crystal.

The fluid-solid coexistence is found when $\Delta W_{fc} = 0$ and $\frac{\delta\Delta W_{fc}}{\delta\rho(\vec{r})} = 0$ are simultaneously satisfied. The minimization of ΔW_{fc} is done with an assumed form of $\rho_c(\vec{r})$. The first term of (2.5) is calculated using a form of $\rho_c(\vec{r})$ which is a superposition of normalized Gaussians centered around lattice sites:

$$\rho_c(\vec{r}) = \left(\frac{\alpha_c}{\pi}\right)^{3/2}\sum_i \exp\left[-\alpha_c\left(\vec{r} - \vec{R}_i^{(c)}\right)^2\right], \tag{2.8}$$

where α_c is the localization parameter and $\vec{R}_i^{(c)}$ are lattice vectors. For other terms of Eq. (2.5) it is convenient to use Eq. (2.7) for $\rho_c(\vec{r})$. The order parameters ρ_K that appear in (2.7) are related to α_c as

$$\rho_K = \rho_c \exp[-K^2/4\alpha_c]. \tag{2.9}$$

B. Solid-solid transition

At the solid-solid phase boundary, the phase that has lower density will be referred to as low density crystal (LDC) and the one that has higher density as high density crystal (HDC); letters l (for LDC) and h (for HDC) will be used to indicate quantities of these phases.

Let the single-particle density distribution of the LDC be expressed in a Fourier series and in the superposition of normalized Gaussians as

$$\rho_l(\vec{r}) = \rho_l + \sum_{K\neq 0}\rho_K e^{i\vec{K}\cdot\vec{r}} \quad \text{and}$$

$$\rho_l(\vec{r}) = \left(\frac{\alpha_l}{\pi}\right)^{3/2}\sum_i e^{-\alpha_l(\vec{r} - \vec{R}_i^{(l)})^2} \quad \text{with} \quad \rho_K = \rho_l e^{-\frac{K^2}{4\alpha_l}}, \tag{2.10}$$

and for the HDC as

$$\rho_h(\vec{r}) = \rho_h + \sum_{G\neq 0}\rho_G e^{i\vec{G}\cdot\vec{r}} \quad \text{and}$$

$$\rho_h(\vec{r}) = \left(\frac{\alpha_h}{\pi}\right)^{3/2}\sum_i e^{-\alpha_h(\vec{r} - \vec{R}_i^{(h)})^2} \quad \text{with} \quad \rho_G = \rho_h e^{-\frac{G^2}{4\alpha_h}}, \tag{2.11}$$

where $\rho_h = \rho_l(1+\Delta\rho^*)$, ρ_l and ρ_h are average densities of the LDC and the HDC, respectively, and $\Delta\rho^*$ is the relative change in density at the transition. $\vec{K}$ and $\vec{G}$ are RLVs and ρ_K and ρ_G are order parameters. α_l and α_h are localization parameters.

The difference in the grand thermodynamic potential of these phases is expressed as

$$\Delta W_{lh} = W_l - W_h = A[\rho_h] - A[\rho_l] - \beta\mu_h \int d\vec{r}\,\rho_h(\vec{r}) + \beta\mu_l \int d\vec{r}\,\rho_l(\vec{r}), \tag{2.12}$$

where $A[\rho_h]$ and μ_h are reduced free energy and chemical potential of the HDC and $A[\rho_l]$ and μ_l are those of the LDC.

The expressions for $A[\rho_h]$ and $A[\rho_l]$ are found from functional integrations of (2.3). The ideal gas part, as stated above, is found analytically. For evaluation of the symmetry conserving part we choose a homogeneous system of density ρ_l (the same as the average density of the LDC), chemical potential μ_0 which, in general, is different from μ_l and μ_h, and the reduced free energy $A(\rho_l)$, as a reference system. The functional integration of (2.3) gives following expression for $A[\rho_l]$:

$$A[\rho_l] - A(\rho_l) = \int d\vec{r}\left[\rho_l(\vec{r}) ln\frac{\rho_l(\vec{r})}{\rho_l} - [\rho_l(\vec{r}) - \rho_l]\right] + \beta\mu_0 \int d\vec{r}[\rho_l(\vec{r}) - \rho_l] - \frac{1}{2}\int d\vec{r}_1 \int d\vec{r}_2[\rho_l(\vec{r}_1) - \rho_l] \times [\rho_l(\vec{r}_2) - \rho_l]c^{(0)}(r,\rho_l) - \int d\vec{r}_1 \int d\vec{r}_2[\rho_l(\vec{r}_1) - \rho_l][\rho_l(\vec{r}_2) - \rho_l]\bar{c}_l^{(b)}(\vec{r}_1,\vec{r}_2), \tag{2.13}$$

where

$$\bar{c}_l^{(b)}(\vec{r}_1,\vec{r}_2) = 2\int_0^1 d\lambda(1-\lambda)\int_0^1 d\xi(1-\xi)c_l^{(b)}(\vec{r}_1,\vec{r}_2;\lambda\rho_l,\xi\rho_K). \tag{2.14}$$

In writing (2.13) use has been made of the relation [4]

$$\ln(\rho_l\Lambda) - c^{(1)}(\rho_l) = \beta\mu_0, \tag{2.15}$$

where $c^{(1)}(\rho_l)$ is the one-particle direct correlation function of the reference system and Λ is the cube of the thermal wavelength associated with a particle. A similar expression can also be written for $A[\rho_h]$.

Substituting expressions of $A[\rho_l]$ and $A[\rho_h]$ in (2.12), we get

$$\Delta W_{lh} = \int d\vec{r}\left[\rho_h(\vec{r})\ln\frac{\rho_h(\vec{r})}{\rho_l} - \rho_l(\vec{r})\ln\frac{\rho_l(\vec{r})}{\rho_l} - [\rho_h(\vec{r}) - \rho_l(\vec{r})]\right] - \beta(\mu-\mu_0)\int d\vec{r}[\rho_h(\vec{r}) - \rho_l(\vec{r})] - \frac{1}{2}\int d\vec{r}_1\int d\vec{r}_2\{[\rho_h(\vec{r}_1) - \rho_l][\rho_h(\vec{r}_2) - \rho_l] - [\rho_l(\vec{r}_1) - \rho_l][\rho_l(\vec{r}_2) - \rho_l]\}c^{(0)}(|\vec{r}_2 - \vec{r}_1|,\rho_l) - \int d\vec{r}_1\int d\vec{r}_2[\rho_h(\vec{r}_1) - \rho_h][\rho_h(\vec{r}_2) - \rho_h]\bar{c}_h^{(b)}(\vec{r}_1,\vec{r}_2) + \int d\vec{r}_1\int d\vec{r}_2[\rho_l(\vec{r}_1) - \rho_l][\rho_l(\vec{r}_2) - \rho_l]\bar{c}_l^{(b)}(\vec{r}_1,\vec{r}_2), \tag{2.16}$$

where $\bar{c}_l^{(b)}(\vec{r}_1,\vec{r}_2)$ is defined by (2.13) and

$$\bar{c}_h^{(b)}(\vec{r}_1,\vec{r}_2) = 2\int_0^1 d\lambda(1-\lambda)\int_0^1 d\xi(1-\xi)c_h^{(b)} \times (\vec{r}_1,\vec{r}_2;\lambda\rho_h,\xi\rho_G). \tag{2.17}$$

In writing (2.16) we assumed $\mu_h = \mu_l$, which happens only at the phase boundary. The quantity $\beta(\mu-\mu_0)$ that appears in (2.16) is found from following relation [11],

$$\beta(\mu-\mu_0) = \Delta f(\rho_l,\alpha_l) + \rho_l\left.\frac{\partial\Delta f(\rho_l,\alpha_l)}{\partial\rho_l}\right|_{T,V}, \tag{2.18}$$

where

$$\Delta f(\rho_l,\alpha_l) = \min\left[\frac{1}{N_l}(A[\rho_l] - A(\rho_l))\right] \tag{2.19}$$

and $N_l = V\rho_l$, V being volume of the system. The minimum in (2.19) is found for a given ρ_l by minimizing $\frac{1}{N_l}\{A[\rho_l] - A(\rho_l)\}$ by varying α_l. The minimum found at a particular value of α_l for given ρ_l is $\Delta f(\rho_l,\alpha_l)$ (see Fig. 3).

Equations (2.5), (2.13), and (2.16) are exact but involve DPCFs, $c^{(0)}$ and $c^{(b)}$, which need to be known. Approximation in the theory enters through them. The value of $c^{(0)}(r)$ is found from the integral equation theory which consists of the Ornstein-Zernike (OZ) equation and a closure relation that connects correlation functions with the interparticle potential [11]. For the symmetry broken part of DPCF, $c^{(b)}(\vec{r}_1,\vec{r}_2)$, a perturbative series expressed in powers of order parameters is used [13]. This series involves higher-body direct correlation functions of a homogeneous system of density equal to the average density of the crystal. For example, for LDC the series is written as

$$c_l^{(b)}(\vec{r}_1,\vec{r}_2;[\rho]) = \int d\vec{r}_3 c_3^{(0)}(\vec{r}_1,\vec{r}_2,\vec{r}_3;\rho_l)(\rho_l(\vec{r}_3) - \rho_l) + \frac{1}{2}\int d\vec{r}_3\int d\vec{r}_4 c_4^{(0)}(\vec{r}_1,\vec{r}_2,\vec{r}_3,\vec{r}_4;\rho_l)[\rho_l(\vec{r}_3) - \rho_l][\rho_l(\vec{r}_4) - \rho_l] + \cdots, \tag{2.20}$$

where $c_m^{(0)}$ is m-body direct correlation function of a homogeneous system of density ρ_l and $\rho_l(\vec{r}) - \rho_l = \sum_{K\neq 0}\rho_K e^{i\vec{K}\cdot\vec{r}}$. The values of $c_m^{(0)}$ (for $m \geqslant 3$) are found from the exact

relation [4,11]

$$\frac{\partial^{m-2}c^{(0)}(|\vec{r}_2-\vec{r}_1|,\rho_l)}{\partial\rho^{m-2}}=\int d\vec{r}_3\cdots\int d\vec{r}_m c_m^{(0)}(\vec{r}_1,\ldots,\vec{r}_m,\rho_l). \tag{2.21}$$

The methods for calculating $c_m^{(0)}$ and $c^{(b)}(\vec{r}_1,\vec{r}_2)$ are discussed in detail in Ref. [16] and briefly summarized in Ref. [18]. For most systems of our interest, the first two terms written explicitly in (2.20) are enough to find accurate values of $c^{(b)}(\vec{r}_1,\vec{r}_2)$ [16,17]. With known values of $c^{(0)}$ and $c^{(b)}$, phase boundaries are found from expressions of ΔW given above.

III. CALCULATION OF PHASE BOUNDARIES: RESULTS AND DISCUSSIONS

We report results for a family of inverse power potentials (IPPs);

$$u(r)=\epsilon\left(\frac{\sigma}{r}\right)^n, \tag{3.1}$$

where r is molecular separation and ϵ, σ, and n are potential parameters. The parameter n measures softness of the potential; $n=\infty$ corresponds to a hard sphere and $n=1$ to a one-component plasma. These potentials have a simple scaling property, according to which the density and temperature can be combined to give a single parameter defined as

$$\gamma=\rho\sigma^3(\beta\epsilon)^{3/n}=\rho^*T^{*-3/n}. \tag{3.2}$$

In term of γ the IPPs are written as

$$\beta u(r)=\left(\frac{4\pi}{3}\gamma\right)^{n/3}\frac{1}{r^n}, \tag{3.3}$$

where r is measured in units of $a_0=(3/4\pi\rho)^{1/3}$.

The computational study of phase diagrams of these potentials shows that more repulsive ($n>7$) systems freeze into an fcc crystal whereas soft sphere systems $n\leqslant 7$ freeze into a bcc crystal [7,8,19]. When pressure is increased the bcc crstal transforms to the fcc crystal [7]. The fluid-bcc-fcc triple point occurs at $1/n\backsimeq 0.15$. For $1/n>0.15$, three phases—fluid, bcc, and fcc—are found.

A. Fluid-solid phase boundary

In [16] we calculated the fluid-solid transition parameters for several values of n ranging from ∞ to 4 and found the fluid-bcc-fcc triple point at $1/n=0.158$ which is somewhat higher than the simulation value $1/n=0.150$. Here we repeat the calculation of [16] and include a few more values of n ($\frac{1}{n}=0.17$, 0.20, and 0.225) so that values of the triple point and the phase boundary as a function of softness parameter $\frac{1}{n}$ can be determined accurately. Equation (2.5), after substitution of expression of $\rho_c(\vec{r})$ given by Eqs. (2.7) and (2.8), reduces to

$$\begin{aligned}\frac{\Delta W_{fc}}{N_c}=&\frac{1}{1+\Delta\rho^*}+\left[\frac{3}{2}\ln\left(\frac{\alpha_c}{\pi}\right)-\frac{5}{2}-\ln\rho_f\right]\\&-\frac{1}{2}\rho_c\left(\frac{\Delta\rho^*}{1+\Delta\rho^*}\right)^2\hat{c}^{(0)}(0)-\frac{1}{2\rho_c}\sum_K|\rho_K|^2\hat{c}^{(0)}(K)\\&-\frac{1}{\rho_c}\sum_K\sum_{K_1}\rho_{K_1}\rho_{|-\vec{K}-\vec{K}_1|}\hat{\tilde{c}}^{(K)}\left(\vec{K}_1+\frac{1}{2}\vec{K}\right),\end{aligned} \tag{3.4}$$

where [16,18]

$$\hat{c}^{(0)}(K)=\int d\vec{r}\,c^{(0)}(r)e^{i\vec{K}\cdot\vec{r}},$$

$$\hat{\tilde{c}}^{(K)}\left(\vec{K}_1+\frac{1}{2}\vec{K}\right)=\int d\vec{r}\,\tilde{c}^{(K)}(\vec{r})e^{-i(\vec{K}_1+\frac{1}{2}\vec{K})\cdot\vec{r}}. \tag{3.5}$$

Here N_c $(=\rho_c V)$ is used to divide ΔW, and a_0 $[=(3/4\pi\rho_c)^{1/3}]$ corresponding to solid average density is used to reduce distance r and localization parameter α_c. The function $\frac{\Delta W_{fc}}{N_c}$ is minimized with respect to γ_f, $\Delta\rho^*$, and α_c. It is found that when γ_f is close to the fluid-solid transition, $\frac{\Delta W_{fc}}{N_c}$ develops a minimum at some value of α_c. The value of minimum of $\frac{\Delta W_{fc}}{N_c}$ and of α_c at which this minimum occurs depend on value of $\Delta\rho^*$. We calculated $\frac{\Delta W_{fc}}{N_c}$ as a function of α_c (varying α_c from 15 to 35 at intervals of 0.5) for several values of γ_f in the neighborhood of the expected transition value and for each γ_f for several values of $\Delta\rho^*$. The variation of $\frac{\Delta W_{fc}}{N_c}$ with γ_f, α_c, and $\Delta\rho^*$ is shown in Fig. 1. The lowest value of γ_f for which the condition $\frac{\Delta W_{fc}}{N_c}=0$ is satisfied and the corresponding values of $\Delta\rho^*$ and α_c are taken as the fluid-solid transition parameters [see Fig. 1(c)]. The result has been confirmed from simultaneous solution of equations $\frac{\partial}{\partial\alpha}(\frac{\Delta W_{fc}}{N_c})=0$, $\frac{\partial}{\partial\Delta\rho^*}(\frac{\Delta W_{fc}}{N_c})=0$, and $\frac{\Delta W_{fc}}{N_c}=0$.

Values of localization parameter α_c found for the bcc crystal at the transition point are in the range of 15–17. This may raise question about the accuracy of the ideal gas term (in the square brackets) in Eq. (3.4), which is found by neglecting overlap between the Gaussians of neighboring lattice sites. We evaluated for $\alpha=15$ the contribution arising from the overlap of Gaussians of nearest neighbors in a bcc crystal and found this contribution to be negligible (see the Appendix).

Values of γ_f, γ_c, and the Lindemann parameter L_c (the subscript c stands for fcc for $1/n<0.154$ and for bcc for $1/n\geqslant 0.154$) are given in Table I for few values of $1/n$ and compared with simulation values in Fig. 2. These values of freezing parameters are close to those reported in [16] and in are good agreement with simulation values [7,19]. The fluid-bcc-fcc triple point is now found at $1/n=0.154$, which is slightly lower and closer to the simulation value [7,19] than the value of 0.158 reported in [16].

B. Solid-solid phase boundary (bcc-fcc boundary)

We first use Eq. (2.13) to calculate $\beta(\mu-\mu_0)$ and α_l. After substitution of the Gaussian and Fourier forms of $\rho(\vec{r})$, Eq. (2.13) reduces to

$$\begin{aligned}\Delta f=\frac{A[\rho_l]-A(\rho_l)}{N_l}=&\frac{3}{2}\left[\ln\left(\frac{\alpha_l}{\pi}\right)-1\right]\\&-\ln\rho_l-\frac{1}{2\rho_l}\sum_K|\rho_K|^2\hat{c}^{(0)}(|\vec{K}|)\\&-\frac{1}{\rho_l}\sum_K\sum_{K_1}\rho_{K_1}\rho_{|-\vec{K}-\vec{K}_1|}\hat{\tilde{c}}_l^{(K)}\left(\vec{K}_1+\frac{1}{2}\vec{K}\right).\end{aligned} \tag{3.6}$$

where $\vec{K}$ is a RLV of the bcc crystal.

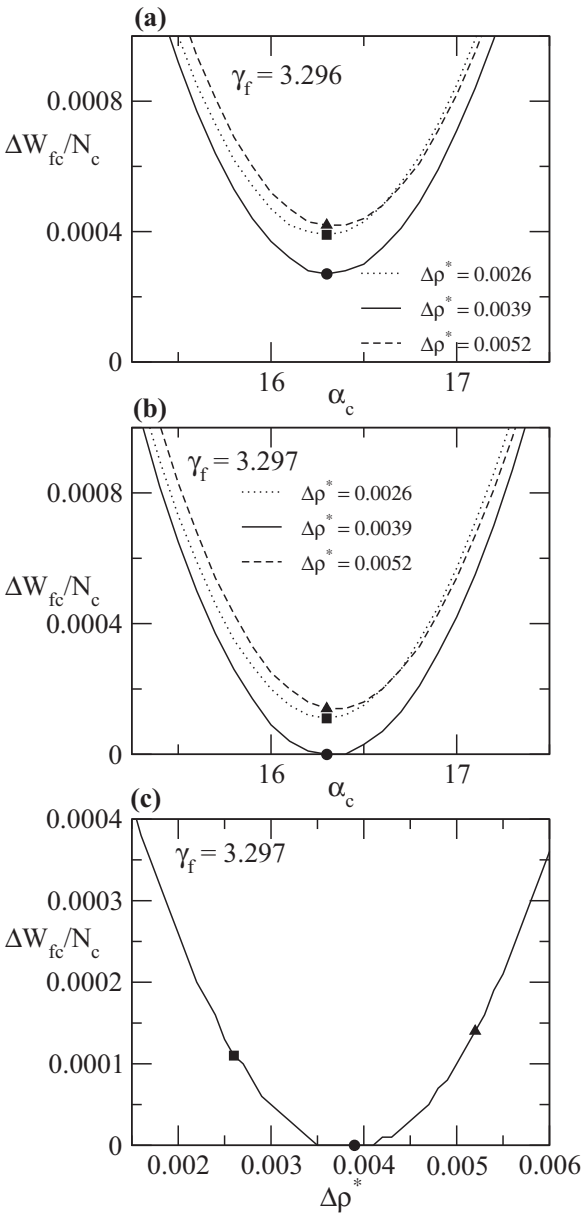

FIG. 1. Variation of $\frac{\Delta W_{fc}}{N_c}$ as a function of α_c and $\Delta\rho^*$ for $1/n = 0.20$ is shown. The minimum of $\frac{\Delta W_{fc}}{N_c}$ and the value of α_c at which this minimum occurs depend on $\Delta\rho^*$. In (a) the variation is shown for $\gamma_f = 3.296$ for three values of $\Delta\rho^*$. in all cases the minimum is greater than zero; the lowest minimum is for $\Delta\rho^* = 0.0039$. In (b) we show the plot for $\gamma_f = 3.297$ where the condition $\frac{\Delta W_{fc}}{N_c} = 0$ is satisfied for $\Delta\rho^* = 0.0039$ and $\alpha_c = 16.3$. In (c) the variation of minimum of $\frac{\Delta W_{fc}}{N_c}$ for $\gamma_f = 3.297$ as a function $\Delta\rho^*$ is shown.

We choose closely spaced values of γ_l starting from a value found at the fluid-bcc transition and calculated Δf as a function of α_l. Note that in this case $\Delta\rho^* = 0$. In Fig. 3 we show variation of Δf as a function of α_l for a few values of γ_l. The function $\Delta f(\gamma_l,\alpha_l)$ that appears in Eq. (2.19) corresponds to minimum value of Δf (shown by a filled circle in Fig. 3) for each γ_l. The value of $\beta(\mu - \mu_0)$ is calculated from Eq. (2.18) from known values of $\Delta f(\gamma_l,\alpha_l)$. This provides us values of $\beta(\mu - \mu_0)$ and α_l for each γ_l used in Eq. (2.16).

TABLE I. Values of transition parameters for the fluid-solid (fcc or bcc) and for the bcc-fcc transitions for IPPs, for some values of softness parameter $1/n$. The subscript c stands for fcc for $1/n <$ 0.154 and for bcc for $1/n \geqslant 0.154$

	fluid-solid			bcc-fcc			
$1/n$	γ_f	γ_c	L_c	γ_{bcc}	γ_{fcc}	L_{bcc}	L_{fcc}
1/7	1.859	1.878	0.120				
2/13	2.040	2.058	0.120				
1/6	2.326	2.342	0.177	2.398	2.406	0.169	0.120
0.170	2.402	2.417	0.177	2.493	2.501	0.169	0.120
0.200	3.297	3.312	0.176	3.460	3.469	0.165	0.120
0.225	4.297	4.310	0.176	4.571	4.578	0.161	0.119
0.250	5.528	5.540	0.175	5.864	5.870	0.160	0.119

The bcc-fcc phase boundary is found from Eq. (2.16), which is rewritten as

$$\begin{aligned}\frac{\Delta W_{l-h}}{N_h} = &\frac{3}{2}\left[\ln\left(\frac{\alpha_h}{\pi}\right) - \frac{1}{(1+\Delta\rho^*)}\ln\left(\frac{\alpha_l}{\pi}\right)\right] \\ &- \frac{\Delta\rho^*}{(1+\Delta\rho^*)}\left[\ln\frac{\rho_h}{(1+\Delta\rho^*)} + \Delta\mu + \frac{5}{2}\right] \\ &- \frac{1}{2}\left[\frac{\Delta\rho^{*2}\rho_h}{(1+\Delta\rho^*)^2}\hat{c}^{(0)}(0) + \frac{1}{\rho_h}\sum_G |\rho_G|^2\hat{c}^{(0)}(|\vec{G}|)\right. \\ &\left. - \frac{1}{\rho_l(1+\Delta\rho^*)}\sum_K |\rho_K|^2\hat{c}^{(0)}(|\vec{K}|)\right] \\ &- \frac{1}{\rho_h}\sum_G\sum_{G_1}\rho_{G_1}\rho_{|-\vec{G}-\vec{G}_1|}\hat{\tilde{c}}_h^{(G)}\left(\vec{G}_1 + \frac{1}{2}\vec{G}\right) \\ &+ \frac{1}{\rho_l(1+\Delta\rho^*)}\sum_K\sum_{K_1}\rho_{K_1}\rho_{|-\vec{K}-\vec{K}_1|} \\ &\hat{\tilde{c}}_l^{(K)}\left(\vec{K}_1 + \frac{1}{2}\vec{K}\right), \end{aligned} \tag{3.7}$$

where $\Delta\mu = \beta(\mu - \mu_0)$ and $N_l = N_h/(1+\Delta\rho^*)$. N_l and N_h are numbers of particles in volume V, respectively, in the LDC (bcc crystal) and the HDC (fcc crystal).

The function $\frac{\Delta W_{l-h}}{N_h}$ is minimized with respect to γ_l, $\Delta\rho^*$, and α_h as the value of α_l is already known. The minimization procedure is same as described above. In Fig. 4 we show the variation of $\frac{\Delta W_{l-h}}{N_h}$ as a function of α_h for different $\Delta\rho^*$ for $1/n = 0.2$. At the transition point $\frac{\Delta W_{l-h}}{N_h} = 0$ [see Fig. 4(c)].

In Table I we give values of γ_l, γ_h, and the Lindemann parameter L. The values of L given in the table for the bcc crystal are 0.176 ± 0.001 along the fluid-bcc boundary and 0.165 ± 0.005 along the bcc-fcc boundary. For the fcc crystal the value of L is 0.12 along both the fluid-fcc and bcc-fcc boundaries. The simulation value of L reported in Refs. [7,20] for the bcc crystal along the fluid-bcc boundary is 0.18, which is in very good agreement with the theoretical value. However, for the fcc crystal the simulation value is 0.15, which is somewhat higher than the theoretical value.

The phase diagram in a plane of softness parameter $1/n$ and the scaled quantity γ is plotted in Fig. 2 and compared with simulation results [7]. From the figure we see that the

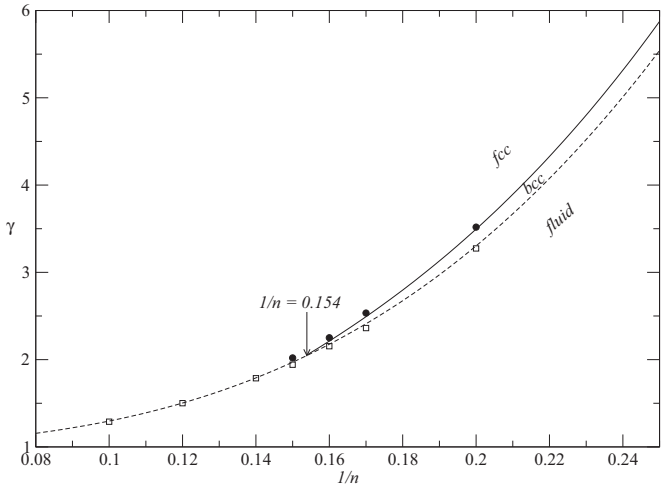

FIG. 2. Phase diagram of systems interacting via IPPs. The dashed line represents the theoretical values for the fluid-solid phase boundary and the full line represents those for the bcc-fcc phase boundary. Open squares and full circles represent, respectively, simulation values [7] for the fluid-solid (fcc or bcc) and the bcc-fcc transition points.

agreement between the two values is good for both the fluid-solid and the solid-solid transition densities. In Fig. 5 we plot for $1/n = 0.2$ the fluid-bcc and bcc-fcc phase boundaries in the ρ^*-T^* plane. For this we used the relation $\gamma = \rho^* T^{*-3/5}$. It is seen from the figure that the stability region of the bcc phase is somewhat underestimated by the theory. The density of a fluid at the fluid-solid transition is marginally higher, and the density of the bcc phase at the bcc-fcc transition is lower than simulation values. However, as the estimated error in the phase transition densities due to limited statistics in simulation is quoted as 3×10^{-2} [7], the difference in the theoretical and simulation values of densities falls within the error bounds. It may also be noted that the change in density at the bcc-fcc transition is considerably smaller than at the fluid-solid transition. This suggests that the bcc-fcc transition is a weak

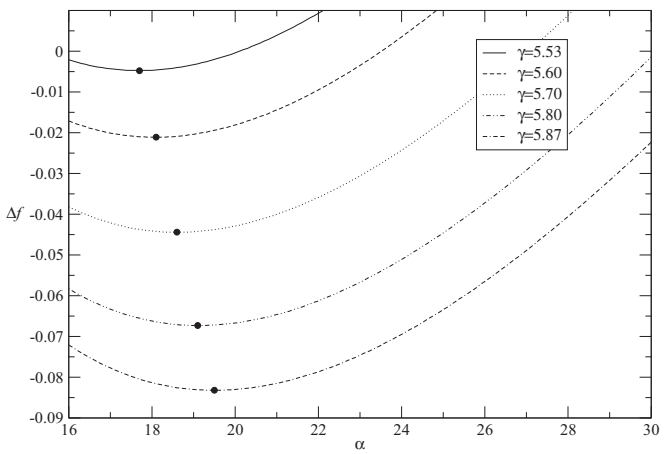

FIG. 3. Variation of Δf as a function of α_l for different γ_l. The minimum found at a value of α_l for each γ_l (shown in figure by full circle) is $\Delta f(\gamma_l,\alpha_l)$ [see Eq. (2.19)].

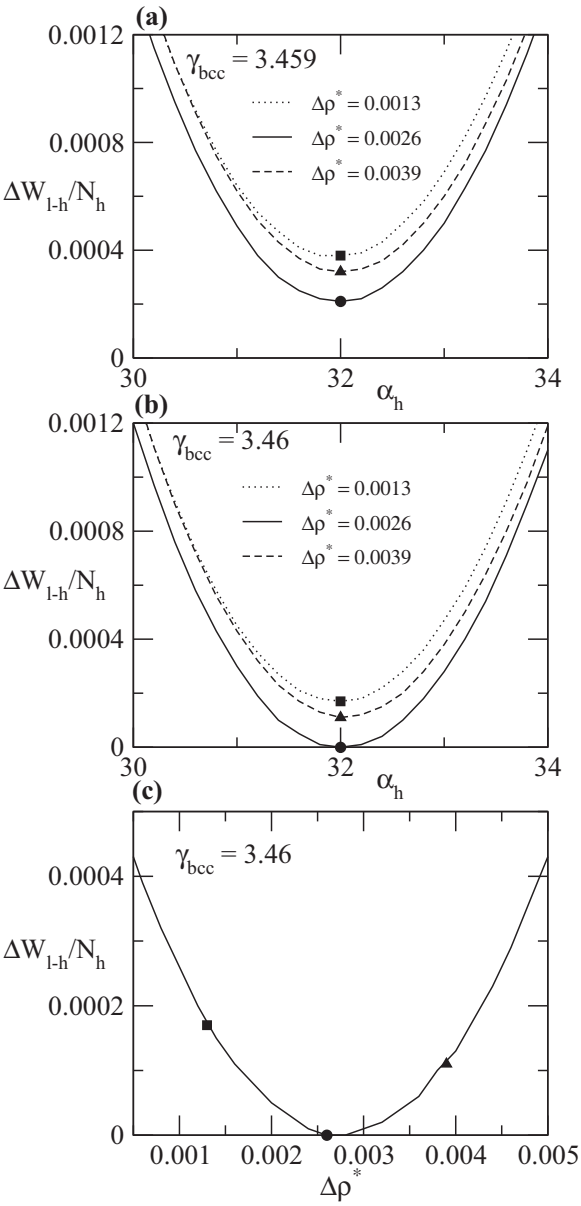

FIG. 4. Variation of $\frac{\Delta W_{l-h}}{N_h}$ as a function of α_h and $\Delta\rho^*$ for $1/n = 0.20$ is shown. In (a) the variation is shown for $\gamma_{bcc} = 3.459$ for three values of $\Delta\rho^*$. The lowest minimum occurs at $\Delta\rho^* = 0.0026$. In (b) the variation is for $\gamma_{bcc} = 3.46$, where the condition $\frac{\Delta W_{l-h}}{N_h} = 0$ is satisfied for $\Delta\rho^* = 0.0026$ and $\alpha_h = 32.0$. In (c) the variation of $\frac{\Delta W_{l-h}}{N_h}$ for $\gamma_{bcc} = 3.46$ as a function of $\Delta\rho^*$ is shown.

first-order transition compared to the fluid-solid transition. In the case of weak the first-order transition the finite-size effects need careful examination even for a sample size as large as that considered in Ref. [7].

Accuracy of theoretical values of the transition parameters depends on accuracy of the input values of $c^{(0)}(r)$ and $c^{(b)}(\vec{r}_1,\vec{r}_2)$. We have used the closure relation of Rogers and Young [21] and numerical procedures which have been found to yield accurate values of correlation functions to calculate values of these functions [16,18]. While $c^{(0)}$ is known to favor fcc structure, it is $c^{(b)}$ which plays a crucial role in stabilizing the bcc structure.

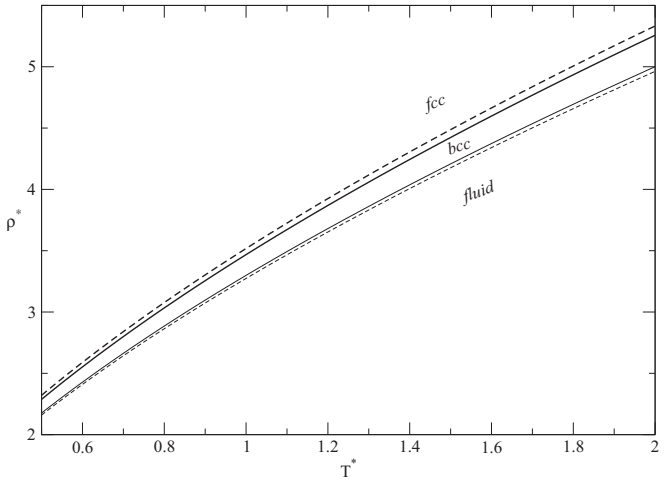

FIG. 5. The density-temperature phase diagram of the IPP for $n=5$ (or $1/n=0.20$). The dashed lines represent simulation values [7] and the full lines theoretical values.

IV. SUMMARY AND CONCLUSION

The theory developed in Refs. [12] and [13] and employed to investigate fluid-nematic and fluid-crystal transitions in two and three dimensions[12–17] is extended here to study crystal-crystal phase transitions. The expressions for the difference in the grand thermodynamic potential of the two coexisting phases at the phase boundary given by Eq. (2.5) for the fluid-crystal and Eq. (2.16) for crystal-crystal phase transitions are exact and involve the symmetry conserving part of DPCF, $c^{(0)}(r,\rho)$, and the symmetry broken part, $c^{(b)}(\vec{r}_1,\vec{r}_2)$. The integral equation theory which consists of the OZ equation and the Roger-Young closure relation [21] has been used to calculate $c^{(0)}(r,\rho)$, $\frac{\partial c^{(0)}(r,\rho)}{\partial\rho}$, and $\frac{\partial^2 c^{(0)}(r,\rho)}{\partial\rho^2}$ for the IPPs. The values of $\frac{\partial c^{(0)}(r,\rho)}{\partial\rho}$ and $\frac{\partial^2 c^{(0)}(r,\rho)}{\partial\rho^2}$ and the factorization ansatz have been used to find values of the three-body direct correlation function $c_3^{(0)}(\vec{r}_1,\vec{r}_2,\vec{r}_3;\rho)$ and four-body direct correlation function $c_4^{(0)}(\vec{r}_1,\vec{r}_2,\vec{r}_3,\vec{r}_4;\rho)$ from exact relations [see Eq. (2.21)]. These equations are solved numerically using an iterative method. The function $c^{(b)}(\vec{r}_1,\vec{r}_2)$ is calculated from Eq. (2.20). As shown in [16], the contribution made by the second term of Eq. (2.20) is very small compared to the first term and needs to be considered only for $n \leqslant 6$.

The agreement found between the calculated phase diagram for systems interacting via the IPPs with the one found from molecular simulations suggests that the theory provides an accurate description of the fluid-solid and the solid-solid transitions and can be used to calculate phase diagrams of systems interacting via known interparticle interactions.

ACKNOWLEDGMENTS

One of us (Y.S.) thanks the Indian National Science Academy, New Delhi for financial support. We thank Prof. T. V. Ramakrishnan for his interest in the problem.

APPENDIX: EVALUATION OF THE IDEAL GAS PART OF THE GRAND THERMODYNAMIC POTENTIAL

The ideal gas part

$$\frac{\Delta W_{id}}{N_c} = \frac{1}{N_c}\int d\vec{r}\left[\rho_c(\vec{r})\ln\frac{\rho_c(\vec{r})}{\rho_f} - (\rho_c(\vec{r})-\rho_f)\right] \quad \text{(A1)}$$

in Eq. (2.5) as well as in Eqs. (2.13)–(2.16) is evaluated using Eq. (2.8) for $\rho_c(\vec{r})$. When the localization parameter α_c is large so that overlap between the Gaussians centered at the lattice sites can be neglected, (A1) is solved to give

$$\frac{\Delta W_{id}}{N_c} = \frac{\rho_c}{1+\Delta\rho^*} + \frac{3}{2}\left(\ln\left(\frac{\alpha}{\pi}\right) - \frac{5}{2} - \frac{2}{3}\ln\rho_f\right). \quad \text{(A2)}$$

However, when α is small the overlap between Gaussians located on neighboring lattice sites cannot be neglected. For the fluid-bcc transition the α value is found to be in the range of 15–17. We evaluate the correction to (A2) arising due to overlap.

If N_c is the number of lattice sites and the origin is located at a lattice site, Eq. (2.8) can be written as

$$\rho(\vec{r}) = N_c\left(\frac{\alpha_c}{\pi}\right)^{3/2}\left[e^{-\alpha_c r^2} + \sum_{1,n} e^{-\alpha_c(\vec{r}-\vec{R}_{1,n})^2} + \sum_{2,m} e^{-\alpha_c(\vec{r}-\vec{R}_{2,m})^2} + \cdots\right], \quad \text{(A3)}$$

where r is confined in a cell of radius $a_0 = (3/4\pi\rho_c)^{1/3}$. $\vec{R}_{1,n}$ are lattice vectors of nearest neighbors (1 indicates first neighbor and n the number) and so on. When we substitute (A3) in first term of (A1) we get

$$\frac{1}{N_c}\int d\vec{r}\left[\rho_c(\vec{r})\ln\frac{\rho_c(\vec{r})}{\rho_f}\right] = \left(\frac{\alpha_c}{\pi}\right)^{3/2}\int d\vec{r}\left[e^{-\alpha_c r^2} + \sum_{1,n} e^{-\alpha_c(\vec{r}-\vec{R}_{1,n})^2} + \cdots\right] \times\left\{\left(\frac{3}{2}\ln\left(\frac{\alpha_c}{\pi}\right) - \alpha_c r^2\right) + \ln\left(1 + e^{-\alpha_c R_1^2}\sum_{1,n} e^{2\alpha_c r R_1\cos(\theta_{1,n}-\theta)} + \cdots\right)\right\}, \quad \text{(A4)}$$

where $\theta_{1,n}$ is the angle of one of the nearest neighbors and θ is the angle of displacement r and R_1 is the magnitude of lattice vectors of nearest neighbors.

Limiting ourselves to the nearest neighbors only we find (A3) has the following contributions:

$$I_1 = \left(\frac{\alpha_c}{\pi}\right)^{3/2} \int d\vec{r}\, e^{-\alpha_c r^2} \left(\frac{3}{2}\ln\left(\frac{\alpha_c}{\pi}\right) - \alpha_c r^2\right), \tag{A5}$$

$$I_2 = \left(\frac{\alpha_c}{\pi}\right)^{3/2} \int d\vec{r}\, e^{-\alpha_c r^2} \ln\left(1 + e^{-\alpha_c R_1^2} \sum_{1,n} e^{2\alpha_c r R_1 \cos(\theta_{1,n}-\theta)}\right), \tag{A6}$$

$$I_3 = \left(\frac{\alpha_c}{\pi}\right)^{3/2} e^{-\alpha_c R_1^2} \int dr\, r^2\, e^{-\alpha_c r^2} \left(\frac{3}{2}\ln\left(\frac{\alpha_c}{\pi}\right) - \alpha_c r^2\right) \int_0^{\pi} d\theta \sin\theta \int_0^{2\pi} d\phi \sum_{1,n} e^{2\alpha_c r R_1 \cos(\theta_{1,n}-\theta)}, \tag{A7}$$

where r is measured in units of a_0.

I_1 when substituted in (A1) gives the expression (A2), and I_2 and I_3 are corrections due to overlap with nearest neighbors.

We calculated the values of I_2 and I_3 for $\alpha_c = 15$ for a bcc lattice and found their values to be negligibly small (at the fourth decimal place).

[1] D. A. Young, *Phase Diagrams of the Elements* (University of California Press, Berkeley, 1991).

[2] T. V. Ramakrishnan and M. Yussouff, Phys. Rev. B **19**, 2775 (1979).

[3] P. A. Monson and D. A. Kofke, in *Advances in Chemical Physics* (John Wiley & Sons, New York, 2007), pp. 113–179, Vol. 115.

[4] Y. Singh, Phys. Rep. **207**, 351 (1991).

[5] A. K. Soper, Science **297**, 1288 (2002); M. Chaplin, Water structure and science: Water phase diagram, http://www1.lsbu.ac.uk/water/water_phase_diagram.html

[6] J. Donohue, *The Structures of the Elements* (John Wiley & Sons, New York, 1974).

[7] S. Prestipino, F. Saija, and P. V. Giaquinta, J. Chem. Phys. **123**, 144110 (2005).

[8] R. Agrawal and D. A. Kofke, Phys. Rev. Lett. **74**, 122 (1995); Mol. Phys. **85**, 23 (1995).

[9] C. N. Likos, B. M. Mladek, D. Gottwald, and G. Kahl, J. Chem. Phys. **126**, 224502 (2007).

[10] Y.-L. Zhu and Z.-Y. Lu, J. Chem. Phys. **134**, 044903 (2011).

[11] J. Hansen and I. McDonald, *Theory of Simple Liquids*, 3rd ed. (Academic Press, Burlington, 2006).

[12] P. Mishra and Y. Singh, Phys. Rev. Lett. **97**, 177801 (2006).

[13] S. L. Singh and Y. Singh, Europhys. Lett. **88**, 16005 (2009).

[14] S. L. Singh, A. S. Bharadwaj, and Y. Singh, Phys. Rev. E **83**, 051506 (2011).

[15] A. Jaiswal, S. L. Singh, and Y. Singh, Phys. Rev. E **87**, 012309 (2013).

[16] A. S. Bharadwaj, S. L. Singh, and Y. Singh, Phys. Rev. E **88**, 022112 (2013).

[17] A. S. Bharadwaj and Y. Singh, J. Chem. Phys. **143**, 124503 (2015).

[18] See Supplemental Material at http://link.aps.org/supplemental/10.1103/PhysRevE.95.032120 for calculation of symmetry conserving and symmetry broken parts of the direct pair correlation function.

[19] R. L. Davidchack and B. B. Laird, Phys. Rev. Lett. **94**, 086102 (2005).

[20] F. Saija, S. Prestipino, and P. V. Giaquinta, J. Chem. Phys. **124**, 244504 (2006).

[21] F. J. Rogers and D. A. Young, Phys. Rev. A **30**, 999 (1984).